Supplementary Materials for

Mutations in the promoter of the telomerase gene *TERT* contribute to tumorigenesis by a two-step mechanism

Kunitoshi Chiba[1,2], Franziska K. Lorbeer[1,2], A. Hunter Shain[3], David T. McSwiggen[1], Eva Schruf[1], Areum Oh[4], Jekwan Ryu[4], Xavier Darzacq[1], Boris C. Bastian[3] and Dirk Hockemeyer[1]*

Affiliations:

[1] Department of Molecular and Cell Biology, University of California, Berkeley, Berkeley, CA 94720, USA

[2] equal contribution

[3] Departments of Dermatology and Pathology, Helen Diller Family Comprehensive Cancer Center, University of California, San Francisco, San Francisco, CA 94115, USA

[4] Optical Biosystems, Santa Clara, CA 95050, USA

*Correspondence to: hockemeyer@berkeley.edu

This PDF file includes:

Materials and Methods
Figs. S1 to S8

Other Suplementary Materials for this manuscript includes the following:

Supplemental information 1: Conversion from days after differentiation to PDs

Materials and Methods

hESC culture and genome editing

Genome editing experiments were performed in WIBR#3 hESCs (*31*), NIH stem cell registry # 0079. Cell culture was carried out as previously described (*32*). hESCs engineered to carry a TPM were subcloned and genotyped as previously reported (*20*). Exon2 of *CDKN2A* was deleted using accattctgttctctctggc and cgcggaaggtccctcaggtg as sgRNA target sites. Targeting was confirmed by Southern blotting with using probe amplified from genomic DNA with primers: Fw: (ggggaaatgatgttggcttagaatcct) and Re: (caatgaagtccttcgtcttggtca). TERT and TR were overexpressed by engineering hESCs to express both from the AAVS1 (*20*).

Southern blot analysis was performed as previously described (*33-35*). Combinatorial mutations in the *TERT* promoter were introduced using a two-step scar-less editing approach (*20*). All comparisons were made between the wild-type *TERT* promoter element (wt) or the respective TPMs (-57A/C, -124 C/T, -146C/T) as described previously (*20*). Cells were cultured for more than 90 days after the targeting and no obvious growth defect was observed in the hESCs.

Differentiation to fibroblast-like cells

Fibroblast-like cells were derived from embryoid bodies (EBs). To form EBs, hESC colonies were grown on petri dishes in fibroblast medium (DMEM [Lifetech]) supplemented with 15% fetal bovine serum [Lifetech], 1 mM glutamine [Lifetech], 1% non-essential amino acids [Lifetech], and penicillin/streptomycin [Lifetech]). After 9 days, EBs were transferred to tissue culture dishes to attach for 6 days. Fibroblast-like cells were passaged with Trypsin EDTA ([Lifetech], 0.25%), triturated into a single-cell suspension and plated on tissue culture dishes.

Growth curve for fibroblasts

Cells were trypsinized, counted and plated at a density of 250,000 cells per 10 cm dish. Medium was changed every 3-4 days and cells were passaged every 5-8 days. Growth curves are presented by plotting cumulative PD against days after differentiation. Most data analysis shown is in reference to the time after differentiation. Supplemental

information table 1 lists the corresponding cumulative PDs for all cell lines at each time point (Fig. 2B-D, Fig. S2E, S5A, S5D, S7C and Fig. 4E). PDs of experiments initiated at a given time point are extrapolated by adding the PD of the parental cell line at the time point of the manipulation.

Generation of cDNA overexpression cell lines and viral infections

For TERT cDNA overexpression, the expressing vector along with lentiviral packaging vectors Delta-VPR and CMV-VSV-G were transfected into HEK293FT cells using calcium phosphate. For POT1 ΔOB cDNA overexpression, the retroviral plasmid was transfected into Phoenix A cells. Media was changed 12 hr after transfection. The virus-containing supernatant was collected 48 and 72 hr post transfection and passed through a 0.45 μm filter to eliminate cells. Target cells were plated in 10 cm plates in media containing 2 μg/ml polybrene. After infection, virus was removed and cells were selected with puromycin or hygromycin. Cells were validated for protein expression via immunoblotting or telomerase activity assay. To transduce cells with SV40 TAg, fibroblasts were infected with pBABE-SV40 large T-Neo at 55 days (for TPMs cells) or 25 days (for TPMs/E3 cells) after differentiation and selected with neomycin.

qRT-PCR

RNA was extracted with TRIzol [Lifetech] and treated with DNaseI [NEB]. 600 ng RNA were converted to cDNA with the iScript Reverse Transcriptase [BioRad] and random and poly(A) priming. qRT-PCR was performed with KAPA SYBR fast [KAPA Biosystems] in 384-well format with a total reaction volume of 10 μl. 2 μl cDNA from the iScript reaction mixture was used for the detection of TERT mRNA. For measuring the expression levels of all other genes, cDNA was diluted 1:10 and 2 μl were used for qPCR. Relative expression levels were calculated based on Δ/ΔCt and/or ΔCt analysis. qRT-PCR primers used in this study were:

TERT fw (TGTCAAGGTGGATGTGACGG), *TERT rev* (GAGGAGCTCTGCTCGATGAC),

GAPDH fw (CAGTCTTCTGGGTGGCAGTGA), *GAPDH rev* (CGTGGAAGGACTCATGACCA),

OCT4 fw (CGTTGTGCATAGTCGCTGCT), *OCT4 rev* (GCTCGAGAAGGATGTGGTCC),

COL1A1 fw (GTCACCCACCGACCAAGAAACC), *COL1A1 rev* (AAGTCCAGGCTGTCCAGGGATG),

GABPα fw (CATCAATGAACCAATAGGCAAT), *GABPα rev* (GGTCAAATAAACTTCGTTCTGGA), *SV40 TAg fw* (GGTGGGTTAAAGGAGCATGA), *SV40 TAg rev* (TAGTGGCTGGGCTGTTCTTT) *CDKN2A ex2 fw* (CAACGCACCGAATAGTTACGG) *CDKN2A ex2 rev* (ACCAGCGTGTCCAGGAAG)

Telomeric repeat amplification protocol

PCR-based telomeric repeat amplification protocol (TRAP) was performed as previously described using TS (AATCCGTCGAGCAGAGTT) and ACX (GCGCGGCTTACCCTTACCCTTACCCTAACC) for amplification of telomeric repeats and TSNT (AATCCGTCGAGCAGAGTTAAAAGGCCGAGAAGCGAT) and NT (ATCGCTTCTCGGCCTTTT) as an internal control (*22*). Cell extract was generated using hypotonic lysis buffer (20 mM HEPES, 2 mM $MgCl_2$, 0.2 mM EGTA, 10% Glycerol, 1 mM DTT, 0.1 mM PMSF) supplemented with 0.5% CHAPS and samples were normalized using the Bradford assay (BioRad). 200 ng of total protein were used for detection of fibroblasts telomerase activity. For hESCs and cancer cell lines, a series of diluted lysate, 200, 40 and 8 ng was used. Throughout the figures, the same hESCs WT lysate was used as a standard. The TRAP products were resolved on a 10% polyacrylamide /1xTAE gel. Dried gels were visualized by phosphor imaging.

Immunoblotting

Protein samples were extracted by hypotonic lysis, normalized for protein concentration and mixed with Laemmli buffer. After heating to 95 °C for 5 min they were resolved by SDS-PAGE. The protein was then transferred to nitrocellulose membrane and subsequently incubated with mouse α-tubulin (1:20000, DM1A [Calbiochem]) and mouse α-Myc (1:20000, [Santa Cruz]) in 4% nonfat milk [Carnation] in TBS-T buffer (150 mM NaCl, 50 mM Tris pH 7.5, 0.1% Tween 20) overnight at 4 °C. The membrane was washed in TBS-T and incubated with goat α-mouse HRP (1:5000, [BioRad]) in 4% nonfat milk in TBS-T for 1 hr at room temperature. After washing with TBS-T, the membrane was visualized using ECL.

Detection of telomere length

Genomic DNA was prepared as described previously (*36*). Genomic DNA was digested with MboI, AluI and RNaseA overnight at 37 °C. The resulting DNA was normalized and 2 μg of DNA was run on 0.75% agarose [Seakem ME Agarose, Lonza], dried under vacuum for 2 hr at 50 °C, denatured in 0.5 M NaOH, 1.5 M NaCl for 30 min, shaking at 25 °C, neutralized with 1 M Tris pH 6.0, 2.5 M NaCl shaking at 25 °C, 2x for 15 min. Then the gel was pre-hybridized in Church buffer (1% BSA, 1 mM EDTA, 0.5M $NaP0_4$ pH 7.2, 7% SDS) for 1 hr at 55 °C before adding a ^{32}P-end-labeled $(T_2AG_3)_3$ telomeric probe. The gel was washed 3x 30 min in 4x SSC at 50 °C and 1x 30 min in 4x SSC + 0.1% SDS at 25 °C before exposing on a phosphorimager screen. Mean telomere length was quantified as described previously (*37*) using the following equation: Mean telomere length = $\Sigma(OD_i \times L_i)/ \Sigma(OD_i)$. OD_i = optical density at position i, L_i= telomere length at position i. To exclude skewing by MEF telomeres, signals above 23 kb were not incorporated into the quantification. Normalized pixel intensity showing the accumulation of short telomeres was calculated by quantifying pixel intensity and normalizing to the area under the curve for each lane using ImageJ and Prism7.

Fusion PCR

Fusion PCR was performed as previously described (*23, 38*) with the following modifications. Briefly, genomic DNA was extracted using phenol chloroform following overnight proteinase K digestion. Isolated DNA was solubilized by EcoRI and RNaseA digestion and phenol chloroform extracted followed by ethanol precipitation. Purified DNA was resolved in TE buffer and quantified. 100 ng of digested DNA were used per 25 µl Failsafe PCR reaction mix (Buffer H) with mixed primers of XpYpM (ACCAGGTTTTCCAGTGTGTT), 17p6 (GGCTGAACTATAGCCTCTGC) and 21q1 (CTTGGTGTCGAGAGAGGTAG). PCR was conducted at the following condition [95 °C for 2 min, (95 °C for 15 sec, 58 °C for 20 sec, 68 °C for 9 min) x35 cycles, 75 °C for 5 min]. PCR products were detected by southern blotting using probes amplified with the following primers: 17p probe: 17p7(CCTGGCATGGTATTGACATG) and 17p2 (GAGTCAATGATTCCATTCCTAGC), XpYp probe: XpYpE2 (TTGTCTCAGGGTCCTAGTG) and XpYpB2 (TCTGAAAGTGGACC(A/T)ATCAG).

Telomeric and centromeric fluorescence in situ hybridization in FFPE samples from patients with melanoma

Tissue sections were deparaffinized with histoclear and rehydrated through a graded alcohol series. They were placed in deionized water followed by permeabilization in water with 0.1% Tween-20 for 2 min. Slides were then placed in 10mM sodium citrate pH 6.5 at 85 °C for 15 min. After rinsing with water, they were treated with 0.4% pepsin for 10 min (pre-warmed to 37 °C). Following another water rinse, slides were dehydrated in a graded alcohol series and air-dried. 100 µl of hybridization buffer (70% formamide, 1 mg/ml blocking reagent [Roche], 10 mM Tris-HCl, pH 7.2, PNA probes [TelC-Cy3, CenpB-Cy5, PNA Bio]) were applied to each section and denaturation was performed by incubation at 75 °C for 10 min. Slides were then moved to a dark container for incubation for 2 hr at room temperature. Slides were washed 3 times in wash buffer (70% formamide, 10 mM Tris-HCl, pH 7.2), followed by 3 washes with PBS. To stain DNA, DAPI (100 ng/mL) was added to the second of the PBS washes.

Image analysis

Image analysis was performed using custom written scripts in Matlab (Mathworks). First, individual high-resolution fields of view were stitched together to generate a single high-resolution file of the tissue sample for each channel: DAPI (nucleus), Cy3 (telomere), and Cy5 (centromere). ROIs were generated by hand to identify relevant tissue types within the images. Individual spots in the Cy3 or Cy5 channels were identified using an adaptation of the MTT detection algorithm, based on maximum likelihood fitting to a two-dimensional Gaussian (*39*). Because of the large size of each image, the stitched high-resolution image was subdivided into 512-by-512 pixel boxes for analysis by MTT, and the detected spots mapped back into the original spatial coordinates. For both channels, the following detection parameters were used: NA: 1.4; detection box: 9 pixels; error rate: 3; deflation loops: 0.

Synthetic Aperture Optics (SAO) reconstruction in StellarVision instrument can introduce periodic structures into low- or homogenous-signal areas of an image (*40*). In order to ensure that only bona fide telomere or centromere spots were being counted, a number of additional filters were applied. First, spot detection was confined only to annotated ROIs. Second, a binary mask was generated using the DAPI channel to only count and include spots that fell within a nucleus. Third, a signal intensity threshold was applied to all detections to remove any detections stemming from

periodic fluctuations in the image background. Intensity thresholds varied from patient to patient, but were held constant for all the images analyzed form the same hybridization. Using these steps, a list of high confidence spots was generated for the telomere channel and the centromere channel. The centromere channel was included in the analysis as an internal normalization for the telomere signal, particularly in order to control for differences in staining and fluorescence signal between tissue types and to control for changes in illumination intensity across a field of view. The closest n centromere spots were identified using 'knnsearch' functions in order to generate a normalized telomere signal for each detected telomere spot. Normalized telomere signal was determined as the telomere intensity divided by the median of those 10 closest centromeres.

A random subsampling was performed to compare telomere lengths between different tissue types within a given sample, and to make an estimate of the magnitude of difference between telomeres in the melanoma and nevus. 50 telomeres from each tissue were randomly sampled, the median calculated, and the signals compared as the ratio between the two. This random resampling was performed for 10,000 iterations with replacement. In the null hypothesis, the two sampled populations would have similar spot intensities, and thus the ratio of the two would be centered around unity.

Statistics

All numerical results are presented as mean and SEM of at least three independent biological or experimental replicates unless stated otherwise. Statistical significance between experimental and control groups was assessed by a two-tailed unpaired Student's *t*-test. A confidence coefficient of 0.05 was used for all tests.

Patient information and data availability

Case 1: Age 52, female, melanoma on posterior shoulder

Case 2: Age 64, male, melanoma on lower back

Case 3: Age 78, male, melanoma on scalp

Case 4: Age 37, male, melanoma on axillary vault

Patient sequencing data is available within the Short Read Archive with the accession number SRP113411. Authors can confirm that all other relevant data are included in the paper and or its supplementary information files. The research was approved by the UCSF human research protection program (institutional review board #11-07951).

Inferred genetic evolution

Phylogenetic trees were constructed as previously described in (*7*). The sequence analysis of Case 2 has been previously reported as Case 9 in (*7*).

Code availability

MATLAB code used for image analysis is available under https://gitlab.com/tjian-darzacq-lab other data are available from the corresponding author.

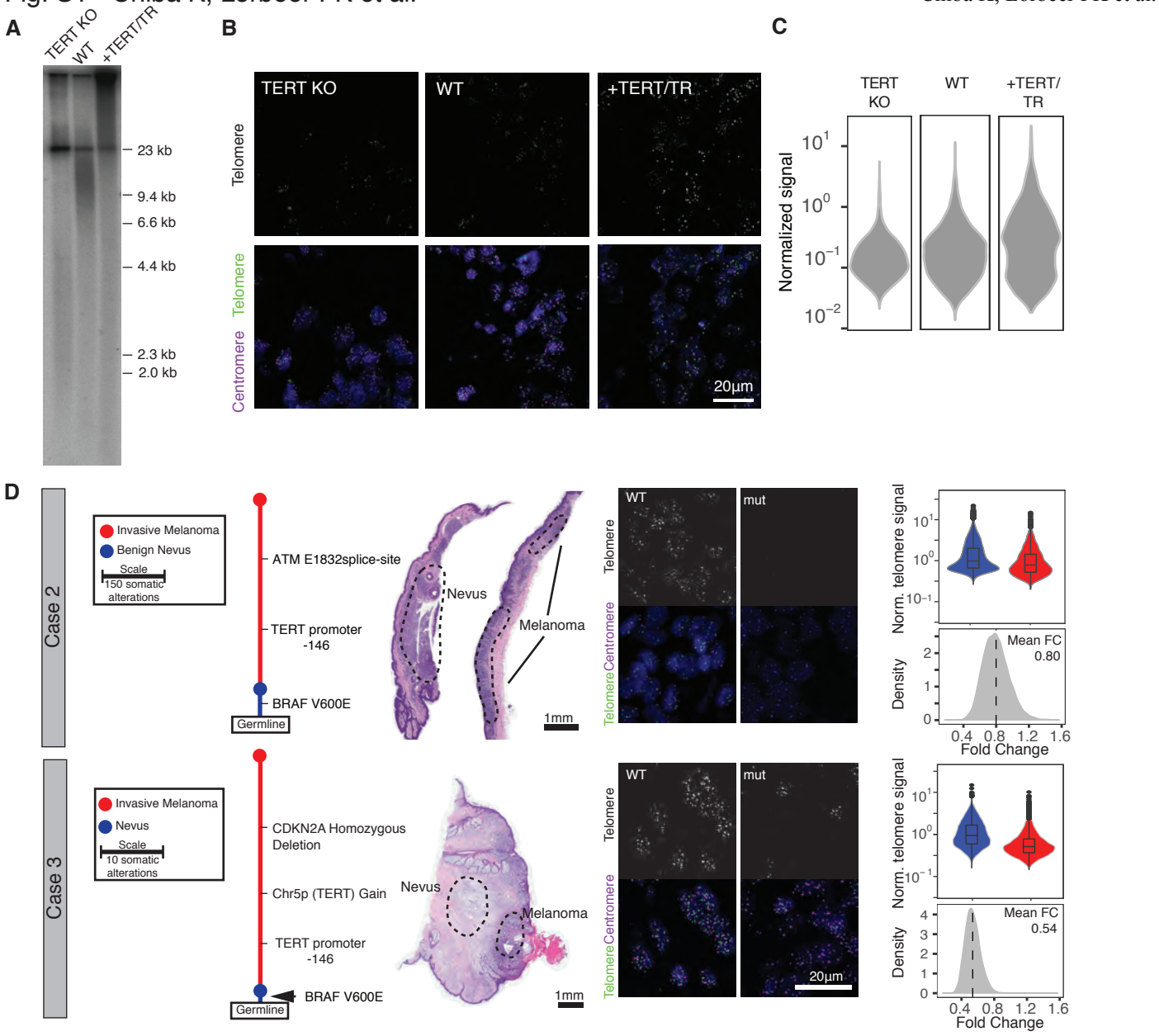

Fig. S1: Structured illumination microscopy allows for quantitative comparison of telomere length
(A) Telomere restriction fragment analysis of telomere length analysis of hESCs of different telomere length. (B) Magnification of structured illumination FISH images of the same hESCs fixed and embedded in paraffin (DAPI = blue, telomere FISH = green, centromere FISH = magenta). (C) Quantitative analysis of telomeric and centromic signal accurately depicts telomere length differences in the analyzed hESCs. (D) Panels as described in Fig. 1: The genetic evolution of each progression case, rooted at the germline, shows how each case evolves from a wild-type nevus to a melanoma with TPM (nevus in blue, melanoma in red). Adjacent is the H&E staining of the analyzed sections of each case (Scale bar 1mm). Magnification of the FISH image resolving individual telomere and centromere spots in nevus/melanoma area (DAPI = blue, telomere = green, centromere = magenta). TPM status is noted as wild-type (WT) or mutant (mut) (Scale bar 20 μm). Violin plots of normalized telomere signal (telomere/centromere) with an inset boxplot indicating the median and quartiles of the signal. Histograms show the fold change of telomere spot intensity after random sampling (fold change melanoma/nevus).

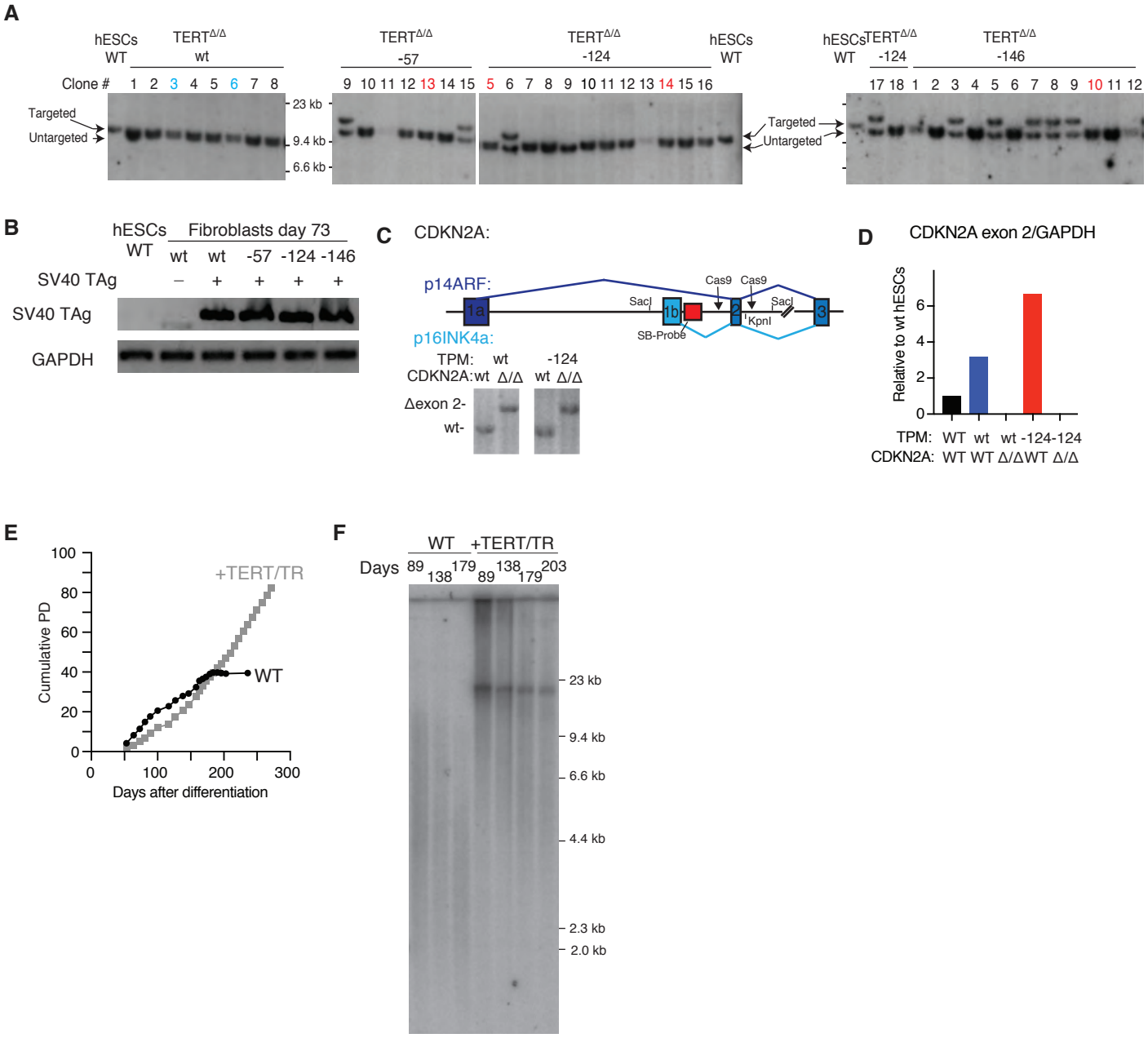

Fig. S2: Genotyping and characterization of cells used in this study

(A) Genotyping of single cell derived isogenic hESC clones with and without TPMs by Southern blotting as previously described in (35). The correctly targeted allele is 11 kb and untargeted is 9.6 kb. The highlighted correctly targeted clones were used for further analysis (wt-6 and -124-14 for checkpoint proficient cells and for the deletion of CDKN2A Δ/Δ; wt-3, -57-13, -124-5 and -146-10 for the SV40 TAg experiments) (B) Expression of SV40 TAg and GAPDH after transduction. (C) Targeting schematic for the generation of CDKN2AΔ/Δ hESCs. Deletion of exon2 of p16 and p14 in the CDKN2A locus was obtained by the simultaneous expression of two Cas9/sgRNAs. For Southern blot analysis, genomic DNA was digested with SacI and KpnI. (D) Confirmation of CDKN2A exon 2 deletion by measuring relative mRNA expression of exon 2. (E) To confirm that arrest of the wild-type cells was due to progressive telomere shortening, TERT and TR, the RNA component of telomerase, were constitutively overexpressed from the AAVS1 locus in hESCs. In fibroblasts, overexpression of telomerase was sufficient to rescue the arrest phenotype and support indefinite proliferation. Growth curves show cumulative PDs over days after differentiation (Wild-type: grey, Overexpression of TERT/TR: black). (F) Telomere length analysis of WT cells and TERT/TR overexpressing cells.

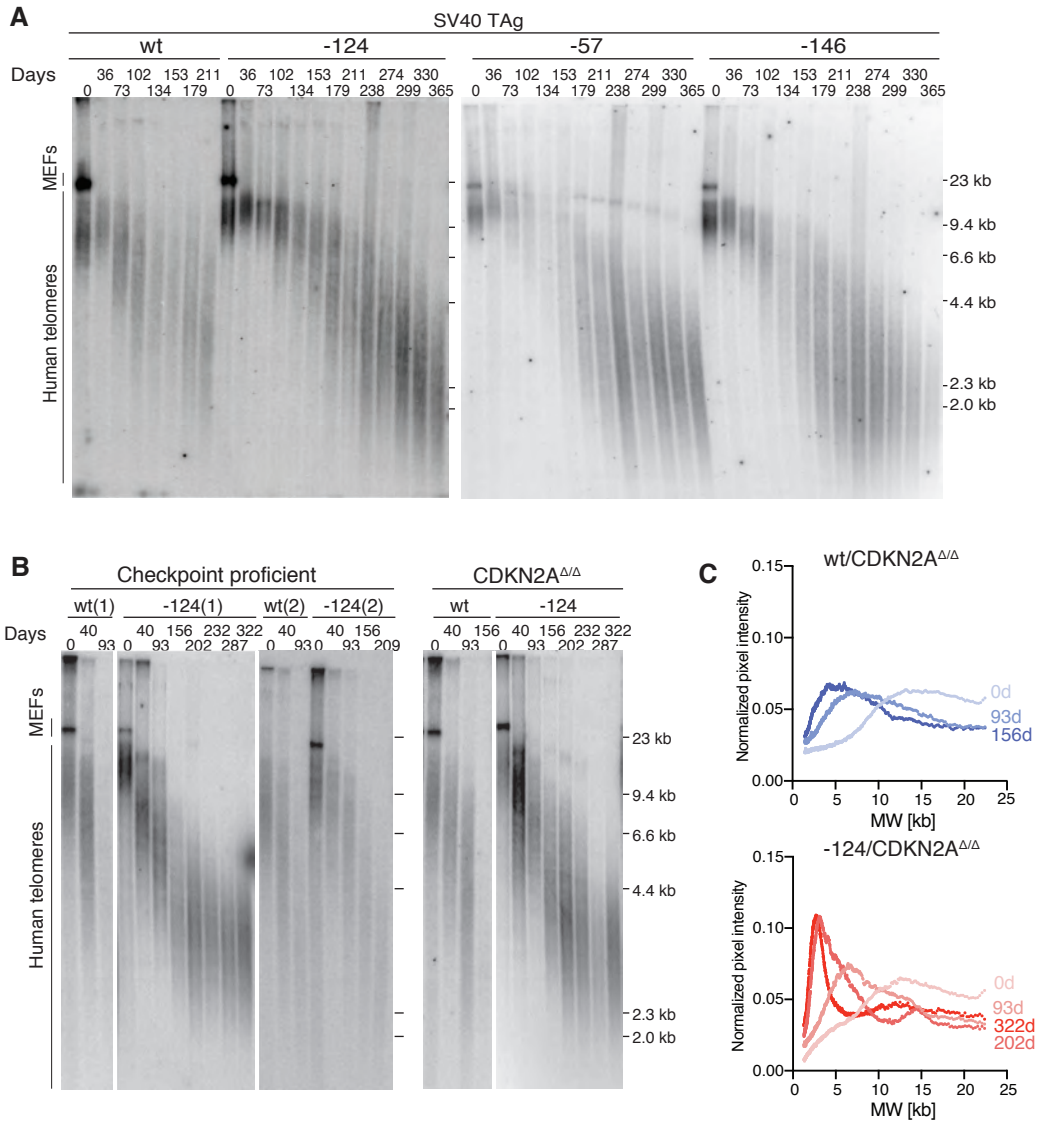

Fig. S3: Telomeres shorten in the presence of TPMs in both checkpoint proficient and deficient cells
(A) Analysis of telomere length in SV40Tag fibroblasts. Day 0 refers to hESCs at the day of differentiation initiation. hESCs are cultured on mouse embryonic fibroblasts (MEFs), the telomeric signal of these MEFs is indicated. Quantification of mean telomere length is shown in Fig. 2E. (B) Analysis of telomere length over time of the cells and experiment shown in Figure 2C and 2D. From the left: Checkpoint proficient cells with or without -124 TPM (two independent -124 TPM clones are shown), CDKN2AΔ/Δ cells with or without -124 TPM. The days post-differentiation are shown above each lane. (C) Accumulation of shorter telomeres over time shown by visualization of telomere length distribution of images shown in panel (B). Quantification of the normalized pixel intensity over molecular weight per lane for the indicated time points after differentiation.

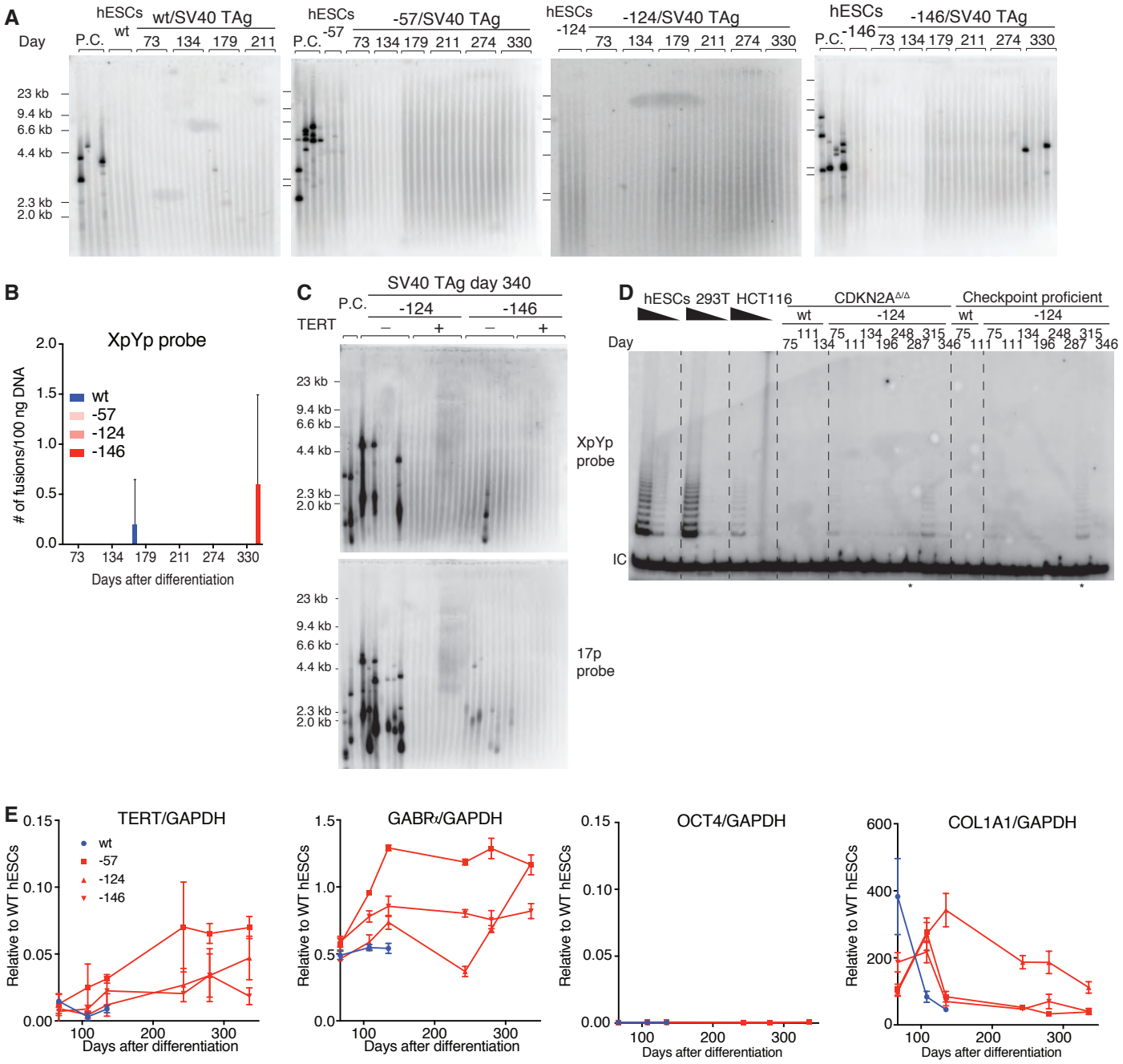

Fig. S4: Gradual telomerase increase is checkpoint independent and via upregulation of TERT mRNA expression
(A) Detection of interchromosomal telomere fusions over time in SV40 TAg fibroblasts by PCR of specific subtelomeric regions. Fusions were detected by probes against the XpYp subtelomeric regions (23). DNA from cells in crisis served as a positive control (P.C.: TERT, p53 and p16 triple knockout fibroblasts cultured into crisis). (B) Quantification of fusion events shown. (C) TERT overexpression suppressed telomeric fusions in TPM cells, demonstrating that fusions are driven by telomere attrition. Telomere fusion PCR was performed in TPM cells with or without overexpression of TERT at day 340. -124 and -146 TPM cells were retrovirally transduced at day 289 with TERT. (D) Telomerase activity assay of the cells shown in Fig. 2C-D over time. IC: internal control for the assay, * indicates time points when telomerase activity becomes detectable. (E) Relative expression levels of TERT, GABPα, OCT4 and COL1A1 mRNA in SV40 Tag cells over time. Expression is relative to WT hESCs and normalized to GAPDH. Error bars show the standard error of the mean (SEM), n = 3.

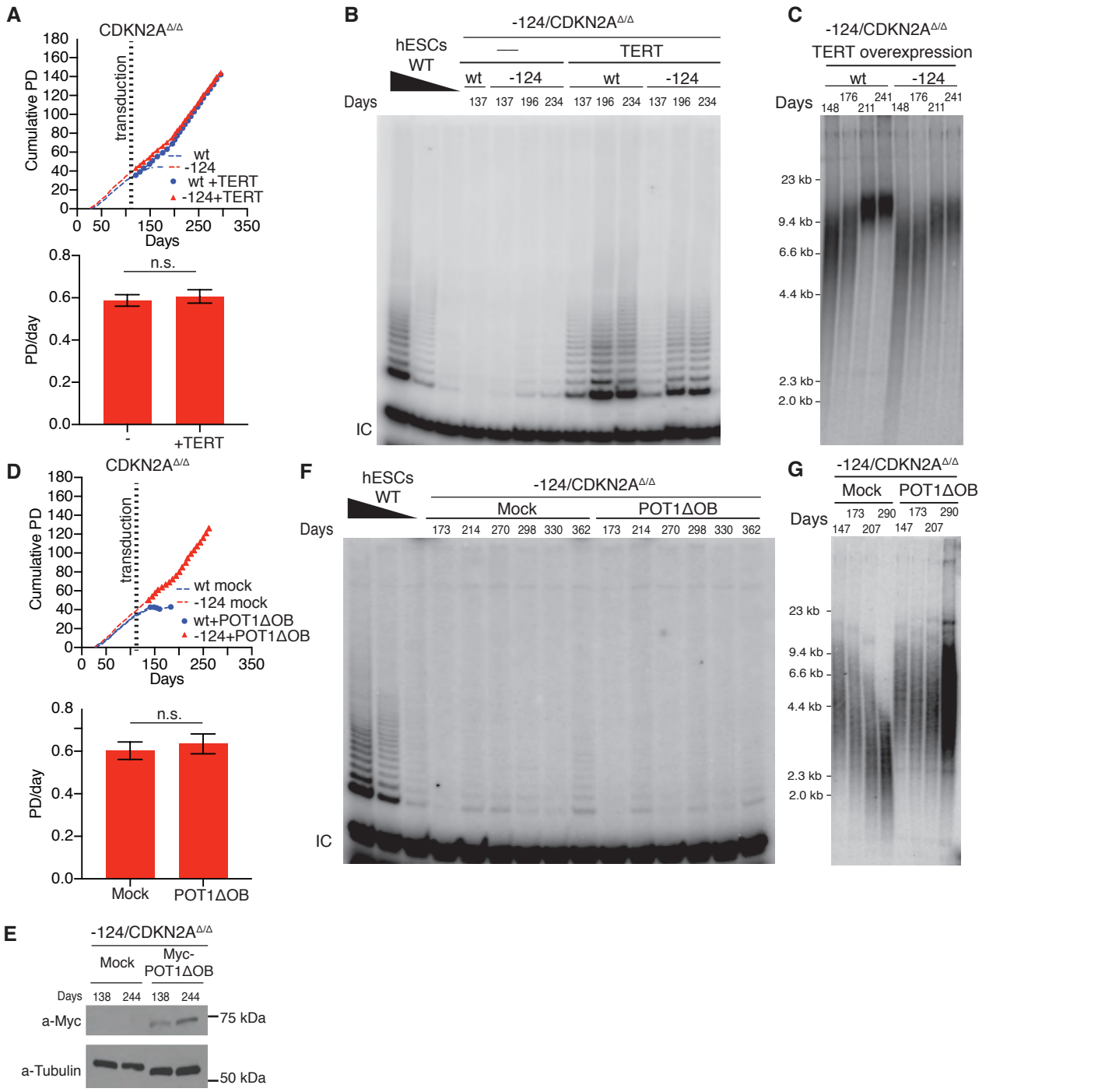

Fig. S5: TERT expression is not limiting for proliferation of TPM cells with sub-threshold telomerase activity
(A) Growth curve and proliferation rate of uninfected and TERT overexpressing cells shown as cumulative PDs over days after differentiation. Cells were infected on day 108 after differentiation (dashed line). PD/day were calculated after each passage between day 129 and 296. Error bars show SEM two-sided student t-test, p = 0.66, n = 24. No significant difference in growth rate was observed indicating that telomerase levels were not limiting for proliferation in TPM cells while telomeres were long. (B) Telomerase activity of TERT overexpressing cells. Uninfected cells were compared with TERT overexpressing cells at 137, 196, and 234 days after differentiation. (C) Telomere length analysis showed telomere elongation by TERT overexpression in wt and -124 TPM cells. (D-G) Telomerase positive cells are highly sensitive to the expression of POT1ΔOB (26), an allele of the shelterin protein POT1 (41), that leads to telomere elongation, but not in telomerase-negative cells. Exploiting this feature, we investigated whether telomere shortening in early

phase was due to complete absence of TERT expression or TERT was expressed at low levels that were insufficient to maintain telomere length. (D) Cumulative PDs of cells retrovirally infected with POT1ΔOB or mock infected cells. No difference in proliferation rate of PD/day was observed after each passage between day 145 and 262. Error bars: SEM, two-sided student t-test, $p = 0.61$, $n = 19$. Cells were infected on day 103 after differentiation. (E) Western blot analysis of retrovirally transduced cells with Myc-POT1ΔOB. (F) Telomerase activity of POT1ΔOB and mock-infected cells at indicated time points after differentiation. (G) Telomere length analysis of POT1ΔOB and mock-infected cells showed expression of POT1ΔOB induced significant telomere elongation in cells with TPMs, indicating telomerase activity that was below the detection limit of our method.

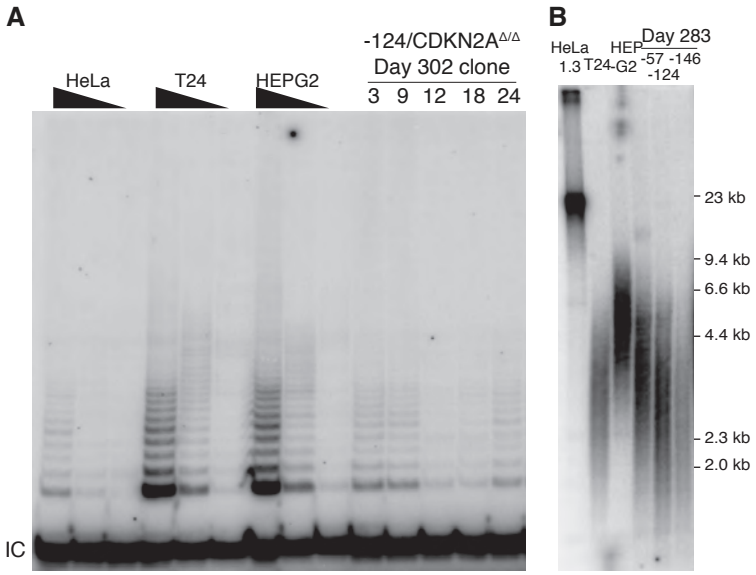

Fig. S6: Telomerase activity and telomere length are not correlated in established cancer cell lines
(A) Comparison of telomerase activity between cancer cell lines and clones of -124 CDKN2AΔ/Δ at day 302. For cancer cell lines, 200, 40, 8 ng of lysate were used for the assay. For -124 CDKN2AΔ/Δ, 200 ng of lysate was used. (B) Comparison of telomere length between the indicated cancer cell lines and SV40 Tag transduced fibroblasts with a TPM at day 283.

A

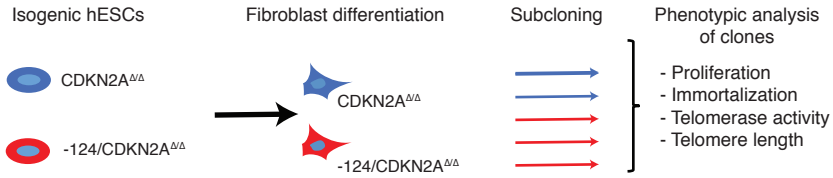

B

Density	Visible outgrowth wt/CDKN2A$^{\Delta/\Delta}$	Visible outgrowth -124/CDKN2A$^{\Delta/\Delta}$
0.5 cells per well	11 of 96	27 of 96
1 cell per well	10 of 96	38 of 96
2 cell per well	17 of 96	62 of 96
4 cell per well	47 of 96	90 of 96

C

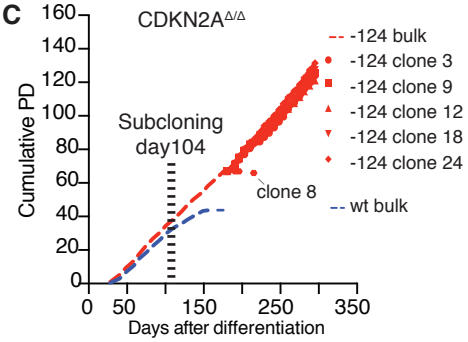

D

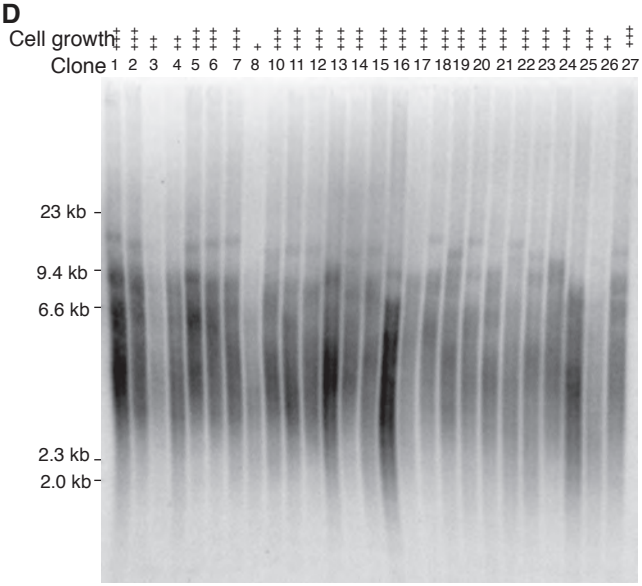

E

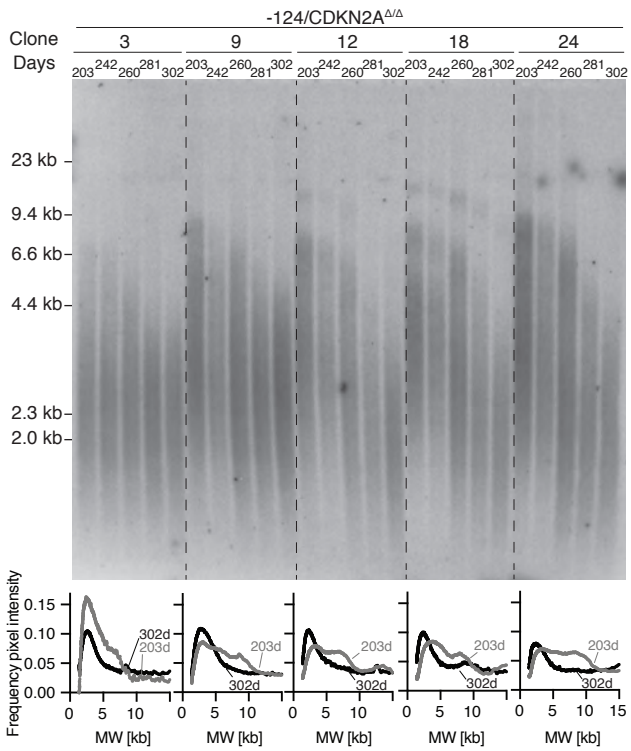

F

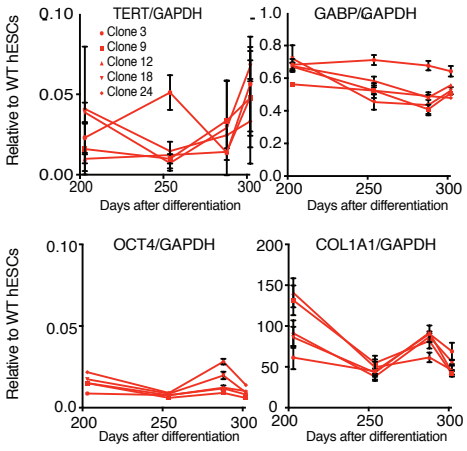

G

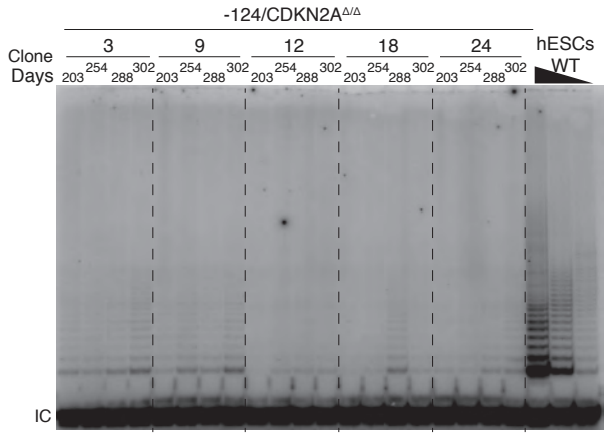

Fig. S7: A large fraction of cells with a TPM are poised to immortalize and exhibit the same telomere length dynamics as the bulk population, yet a small fraction of individual cell clones failed

(A) Experimental overview: To assess the potential of individual cells within a population to stabilize their telomeres and immortalize, we isolated subclones of -124 TPM (CDKN2AΔ/Δ) and wild-type (CDKN2AΔ/Δ) cells at day 104 after differentiation, before the upregulation of telomerase. (B) Table of frequency of successful subcloning by limiting dilution. We isolated 11 clones from wild-type and 27 clones from cells carrying the -124 TPM. Both sets of clones grew in parallel for 45 days before all wild-type clones ceased to proliferate. (C) Telomere length analysis of all TPM clones at day 149. Evaluation of cell growth is indicated above each clone ranging from poor growth (+) to excellent growth (+++). Six cell lines were chosen for long-term analysis. (D) Growth curve showing cumulative PDs over time of the six of the subcloned lines. Five out of six clones proliferated more than 70 PDs beyond the proliferative capacity of wild-type cells. However, one of the six clones (#8), stopped proliferating with morphology and culture characteristics of cells in crisis. (E) Telomere length analysis of the clones analyzed for proliferation. Plotted below the autoradiogram are the telomere length distributions (frequency of pixel intensity over molecular weight) of the earliest and latest time point (Day 203, grey line and 302, black line). (F) Relative expression levels of TERT, GABPα, OCT4, COL1A1 mRNA in each clone between days 203 and 302. Expression was normalized by GAPDH. Error bars show SEM, n = 3. (G) Telomerase activity assay of the TPM -124 clones at indicated time points after differentiation.

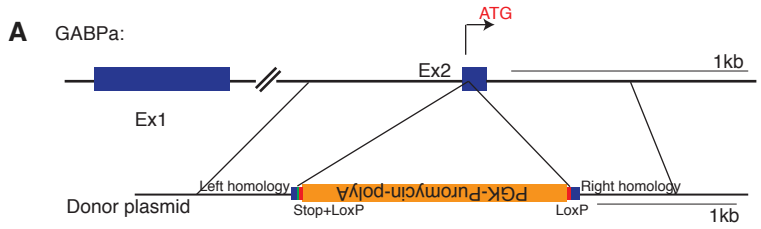

hESCs	# of clones genotyped	# of clones heterozygous targeted	# of clones homozygous targeted
WT	23	12 (52%)	0
TERT$^{\Delta/\Delta}$ wt	18	6 (33%)	0
TERT$^{\Delta/\Delta}$ -57	14	4 (29%)	0
TERT$^{\Delta/\Delta}$ -124	15	5 (33%)	0
TERT$^{\Delta/\Delta}$ -146	14	5 (36%)	0

B

GABPa$^{+/-}$ hESCs clone	Sequence of non-integrated alleles	Status
Reference seq.	cATGACTAAAAGAGAAGCAGAGGAGCTGATA (sgRNA / PAM)	—
WT-9	ATGACTAAAAGAGAAGCAGAGGAGCTGATA	wild type
wt-6	ATGACTAAANGAGAAGCAGAGGAGCTGATA	wild type
-57-4	ATGACTAAANGAGA------GGAGCTGATA	6 bp deletion
-57-18	ATGACTAAAAGAGA---------GCTGATA	9 bp deletion
-57-25	ATGACTAAAAGAGA---------GCTGATA	9 bp deletion
-124-2	ATGACTAAAAGAGAAGCAGAGGAGCTGATA	wild type
-146-15	ATGACTAAANGAGAAGCAGAGGAGCTGATA	wild type
-146-28	ATGACTAAAAGAGA------GGAGCTGATA	6 bp deletion

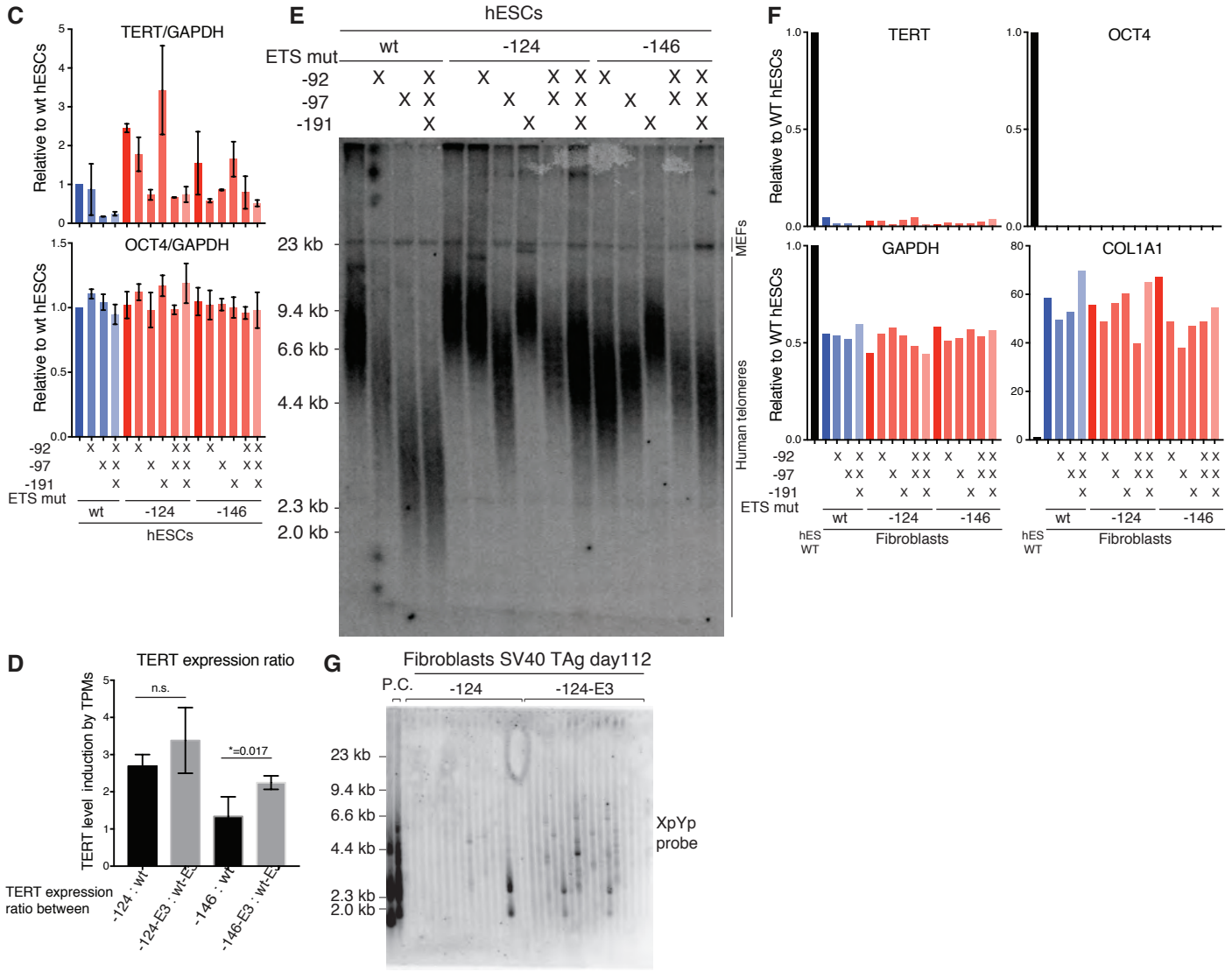

Fig. S8: Modulation of TERT expression by attempted GABPα knockout and mutation of endogenous ETS sites in the TERT promoter

(A) Schematic overview of GABPα knockout strategy and frequency of successful targeting determined by Southern blot genotyping. (B) PCR genotyping of non-integrated alleles of GABPα+/- clones. Note: All alterations of the non-targeted allele are in-frame deletions. These in-frame deletions are expected to retain GABPα function, suggesting an

essential role for GABPα in hESCs. Using an alternative approach, we mutated the three endogenous ETS-factor binding sites in the TERT promoter (E3), which have been proposed as binding sites of the GABPα/β heterodimer. (C) Relative expression levels of TERT and OCT4 for the indicated combinations for mutations in the endogenous ETS sites with or without TPMs. Expression levels are relative to hESCs and normalized to GAPDH. Mutations in the ETS sites decrease TERT expression in wt hESCs, indicting a contribution of these ETS sites to TERT transcription even in the absence of the TPMs. Moreover, the endogenous ETS sites did not act cooperatively but rather additively with the TPMs, as TPMs were able to increase TERT transcription in the presence of the triple ETS mutation.(D) Fold change of TERT expression for the indicated comparisons (Error bars: SEM, two-sided student t-test, n = 3). TPMs can equally upregulate TERT expression in the absence of the endogenous ETS sites. (E) Telomere length analysis of hESCs carrying individual and combinatorial mutations in the endogenous ETS sites with or without TPMs. (F) Relative expression levels of TERT, OCT4, GAPDH and COL1A1 in fibroblasts differentiated from hESCs. Samples were collected at day 21 after differentiation. (G) Telomere fusions detected in -124 and -124 E3 fibroblasts with probe XpYp in subtelomeric regions at day 112.

Supplemental information 1: Conversion from days after differentiation to PDs

Figures 2, 3 and 4 show data as a function of time in days after differentiation. This table lists the respective PDs of each culture at these time points.